Molecular Phylogenetics and Evolution 201 (2024) 108218



Contents lists available at ScienceDirect

Molecular Phylogenetics and Evolution

journal homepage: www.elsevier.com/locate/ympev





Jumping through hoops: Structural rearrangements and accelerated mutation rates on Dendrodoridídae (Mollusca: Nudibranchia) mitogenomes rumble their evolution

Carles Galià-Camps [a,b,*], Tilman Schell [c,d], Alba Enguídanos [b,e], Cinta Pegueroles [b,f], Miquel A. Arnedo [b,e], Manuel Ballesteros [b,e], Ángel Valdés [g,1], Carola Greve [c,d,1]

[a] Centre d'Estudis Avançats de Blanes (CEAB, CSIC), Accés Cala St. Francesc 14, 17300 Blanes, Girona, Spain
[b] Institut de Recerca de la Biodiversitat (IRBio), Universitat de Barcelona, Barcelona, Spain
[c] LOEWE Centre for Translational Biodiversity Genomics (LOEWE-TBG), Senckenberganlage 25, 60325 Frankfurt am Main, Germany
[d] Senckenberg Forschungsinstitut und Naturmuseum, Senckenberganlage 25, 60325 Frankfurt am Main, Germany
[e] Departament de Biologia Evolutiva, Ecologia i Ciències Ambientals. Universitat de Barcelona, Avinguda Diagonal 643, 08028 Barcelona, Spain
[f] Departament de Genètica, Microbiologia i Estadística, Universitat de Barcelona, Avinguda Diagonal 643, 08028 Barcelona, Spain
[g] Department of Biological Sciences, California State Polytechnic University Pomona, 3801 West Temple Avenue, Pomona, CA 91768, USA

ARTICLE INFO

Keywords:
Mollusca
dN/d*S*
Protein modeling
Systematics
Cyto-nuclear discordance

ABSTRACT

The systematics of the family Dendrodoridídae, with only three valid genera, is a challenge for integrative taxonomists. Its members lack hard structures for morphological comparisons and their mitochondrial and nuclear markers provide contradictory phylogenetic signals, making phylogenetic reconstructions difficult. This molecular discordance has been hypothesized to be the result of nuclear pseudogenes or exogenous contamination. However, these hypotheses have not been tested. Here, we assembled the first genome drafts of seven Dendrodoridídae species to investigate the evolutionary processes of this family. Two of the mitogenomes displayed an identical structural rearrangement involving the translocation of three coding genes and five tRNAs, described for the first time in nudibranchs. In addition, we found particularly high d*N* and d*N*/d*S* values and multiple insertions and deletions on the mitochondrial genes of smooth *Dendrodoris*. In contrast, nuclear single-copy ortholog genes showed no such mutational differences. Models of protein structures from mitochondrial genes are conserved, suggesting conserved functionality. Phylogenies using mitogenomic and nuclear data showed that species with rearranged mitogenomes form a clade, although Dendrodoridídae relationships remained unresolved. The present study provides novel evidence for accelerated mutation rates in the mitogenomes of Dendrodoridídae, which presumably have implications on respiratory adaptation, and highlights the importance of using genomic data to unveil rare evolutionary processes, crucial for correctly inferring phylogenies.

1. Introduction

Species can be considered a set of metapopulations that evolve independently, accumulate differences, and eventually become discrete biological units (de Queiroz, 2005). From an evolutionary perspective, the process of speciation involves several factors, with mutation and natural selection being the main drivers (Schluter and Rieseberg, 2022). Some mutations directly affect individual fitness by influencing survival under specific environmental pressures, while others can favor phenotypes through sexual preference (Wellenreuther et al., 2014). Although the barriers can be reproductive or ecological, both processes eventually lead to speciation (Cooney et al., 2017; Marques et al., 2019; Mendelson and Safran, 2021; Teske et al., 2019). Interestingly, gradients of genetic variation can be established during the speciation process, resulting from repeated gene flow between metapopulations and leading to a range of phenotypic traits (Abbott et al., 2013). However, drastic changes at the DNA structural level can also occur suddenly, changing chromosome conformation and the interaction among their respective

* Corresponding author at: Centre d'Estudis Avançats de Blanes (CEAB, CSIC), Accés Cala St. Francesc 14, 17300 Blanes, Girona, Spain.
E-mail address: carles.galia@ceab.csic.es (C. Galià-Camps).
[1] Senior researcher.

https://doi.org/10.1016/j.ympev.2024.108218
Received 17 June 2024; Received in revised form 8 October 2024; Accepted 8 October 2024
Available online 17 October 2024
1055-7903/© 2024 The Author(s). Published by Elsevier Inc. This is an open access article under the CC BY-NC license (http://creativecommons.org/licenses/by-nc/4.0/).

regions, such as chromosome fissions or fusions, or chromosome inversions (de Vos et al., 2020). If the mutated individual is viable, these mutations can hamper reproduction with non-mutated individuals, thus promoting accelerated speciation through chromosome pairing incompatibilities (Řezáč et al., 2018).

Although widely reported, accelerated evolutionary processes driving speciation are rare (Cardini et al., 2007; Nowak et al., 2008). Genomic inversions, the reversal of the orientation of relatively large chromosomal fragments, are among the most commonly described processes for speciation reported in the literature (Fuller et al., 2019; Schluter and Rieseberg, 2022), abruptly creating reproductive barriers resulting from unequal crossover (Fuller et al., 2019; Schluter and Rieseberg, 2022). Other mechanisms of accelerated evolution have been proposed, such as epistasis, which promotes rapid coevolution of interacting genes that can accomplish a high level of genetic differentiation in a few generations (Breen et al., 2012). Furthermore, high mutation rates can produce incompatibilities among individuals of the same species (de Visser et al., 2011; Johnson et al., 2023; Phillips, 2008). Fast-occurring incompatibilities are not exclusive to the nuclear genome, since similar processes can occur in the mitochondrial genome (Burton, 2022; Hill, 2016; Tobler et al., 2019). Cyto-nuclear interactions may play an important role in speciation as genes from both the nuclear and the mitochondrial genomes are required for proper functioning of cellular respiration (Sutovsky, 2019), as well as for an accurate and even distribution of mitochondria during mitosis and meiosis (Ghiselli et al., 2019). Thus, mutations occurring in one of these interacting genomic regions must be repaired or compensated by a counter-mutation as long as fitness is not affected (Hill, 2020). Once the compensation process occurs in a specific lineage, mitochondrial and nuclear mutations can cause incompatibilities with other individuals from the same species (Burton, 2022; Visinoni and Delneri, 2022).

The family Dendrodorididae presents several challenges for integrative taxonomists. The family contains three accepted genera: *Dendrodoris*, the most speciose with 45 species, followed by *Doriopsilla* with 27 species, and the controversial monotypic genus *Cariospilla*. Members of this family lack taxonomically important structures present in most other gastropods, such as the shell, radula, and jaws. Moreover, their mitochondrial and nuclear markers provide contradictory phylogenetic signals (Galià-Camps et al., 2022). Recent phylogenies based on partial cytochrome oxidase I (*cox1*) and ribosomal 16S sequences either placed *Dendrodoris* outside of Nudibranchia (Wollscheidlengeling, 2001), or showed that *Dendrodoris* members displayed extremely long branches (Hallas et al., 2017; Korshunova et al., 2020). Long branches in phylogenies usually reflect distant evolutionary relationships, although they can indicate accelerated evolutionary rates when found in closely related taxa (Omilian and Taylor, 2001). Nevertheless, long branches within *Dendrodoris* have been suspected to be the result of contamination or a pseudogene that happens to resemble the insect's *cox1*, as found with BLAST (Hallas et al., 2017; Korshunova et al., 2020). However, neither the pseudogene nor the contamination hypotheses have ever been tested.

Here, we aim to unravel the evolutionary processes that have led to conflicting results in previous research using *Dendrodoris* mitochondrial gene sequences. To do so, we use low-coverage whole genome sequencing of seven Dendrodorididae species to reconstruct their mitochondrial genomes and generate their first nuclear genome draft assemblies. We evaluate the mitochondrial structure of the seven species and confirm that smooth *Dendrodoris* possess a unique mitogenome among nudibranchs. We test the d*N*, d*S*, and d*N*/d*S* of mitochondrial coding genes and 15 nuclear single-copy ortholog genes, and show that smooth *Dendrodoris* species have suffered from accelerated mutation rates. We validate the functionality of mitochondrial coding sequences by modeling their tertiary structure. We use mitochondrial gene sequences independently and in combination with nuclear single-copy ortholog genes to assess the family phylogenetic relationships. Furthermore, we use genome-wide markers to validate the results of the phylogenetic analyses. Based on the presented results, we discuss the evolutionary processes that may have shaped the mitogenome structure of Dendrodorididae and the phylogenetic relationships of the family. This study presents novel results on drastic changes in molluscan mitogenomic evolutionary processes, discusses the cyto-nuclear interaction, and explores possible respiratory adaptations caused by habitat change.

2. Material & Methods

2.1. Taxon sampling

Seven Dendrodorididae species were collected in shallow waters of Spain (Catalonia) and USA (California and Hawaii) (Supplementary Data 1: Table S1). The sampling was designed to obtain at least two representatives from each of the main *Dendrodoris* morphotypes: smooth *Dendrodoris* (*D. limbata* and *D. temarana*) and tuberculated *Dendrodoris* (*D. tuberculosa*, *D. elongata,* and *D. krusensternii*), as well as *Doriopsilla* (*Do. rarispinosa* and *Do. spaldingi*) (Fig. 1).

2.2. DNA extraction and library preparation

For *Dendrodoris temarana*, DNA was extracted from foot tissue using a customized phenol–chloroform protocol with magnetic beads based on (Mayjonade et al., 2016). The DNA extraction was sent to Novogene (UK) for short read Illumina genome sequencing. The genomic library was prepared with an insert size of 350 bp, and an Illumina NovaSeq 6000 platform (San Diego, CA) was used to sequence 150 bp paired-end reads, aiming for 60 Gb output.

For the remaining *Dendrodoris* and *Doriopsilla* specimens, DNA was extracted from foot tissue using the Gentra Puregene Tissue Kit (QIAGEN) by following the manufacturer's instructions. An initial amount of DNA ranging from 300 to 500 ng was used for library construction using all standard kit reagents from the Illumina DNA prep (M) Tagmentation (Illumina, San Diego, CA), altogether with Illumina commercial indexes (IDT for Illumina DNA/RNA UD Indexes set A, Tagmentation) by following the kit manual instructions. Library preparations (insert size: 350 bp) were sent to Macrogen (Macrogen Korea) for 150 bp paired-end reads sequencing on a HiSeqX platform with 14 Gb output each.

2.3. Data curation, assembly, and annotation

Raw data were submitted to the European Nucleotide Archive (ENA) under the Bioproject PRJEB75450. Low-quality data and adapters were discarded using Trimmomatic 0.39 (Bolger et al., 2014), applying default parameters. For the mitochondrial genome assembly reconstruction, NOVOPlasty v4.3.1 (Dierckxsens et al., 2017) was run for all the individuals using a k-mer size of 21 and the *cox1* gene sequence of each species as seed (Supplementary Data 1: Table S1), except for *D. elongata* as its *cox1* was not available in public databases and we used the *D. krusensternii cox1* instead. The complete mitogenome of *Phyllidia ocellata* (Xiang et al., 2016) (NCBI accession number KU351090) was used as the reference mitogenome for all assemblies (Supplementary Data 1: Table S1). We evaluated the presence of heteroplasmy for each sample with NOVOPlasty, using its respective assembled genome as seed along with the filtered reads of the sample, setting a minimum allele frequency of 0.1. Additionally, to ensure the quality of our mitogenome assemblies, we mapped the filtered reads of each specimen back to their respective mitochondrial genome assembly with bwa v0.7.1 *mem* (Li and Durbin, 2009), and visualized the coverage with ggplot2 v3.5.0 (Wickham et al., 2016). MITOS2 (Donath et al., 2019), implemented in the GALAXY web server https://usegalaxy.eu/, was used to annotate ribosomal RNAs (rRNA), coding sequences (CDS), and transfer RNAs (tRNA), which were subsequently visualized and manually curated using Geneious Prime 2022.1.1 (Biomatters Ltd).

SPAdes v3.11.0 (Prjibelski et al., 2020), was run on the filtered reads

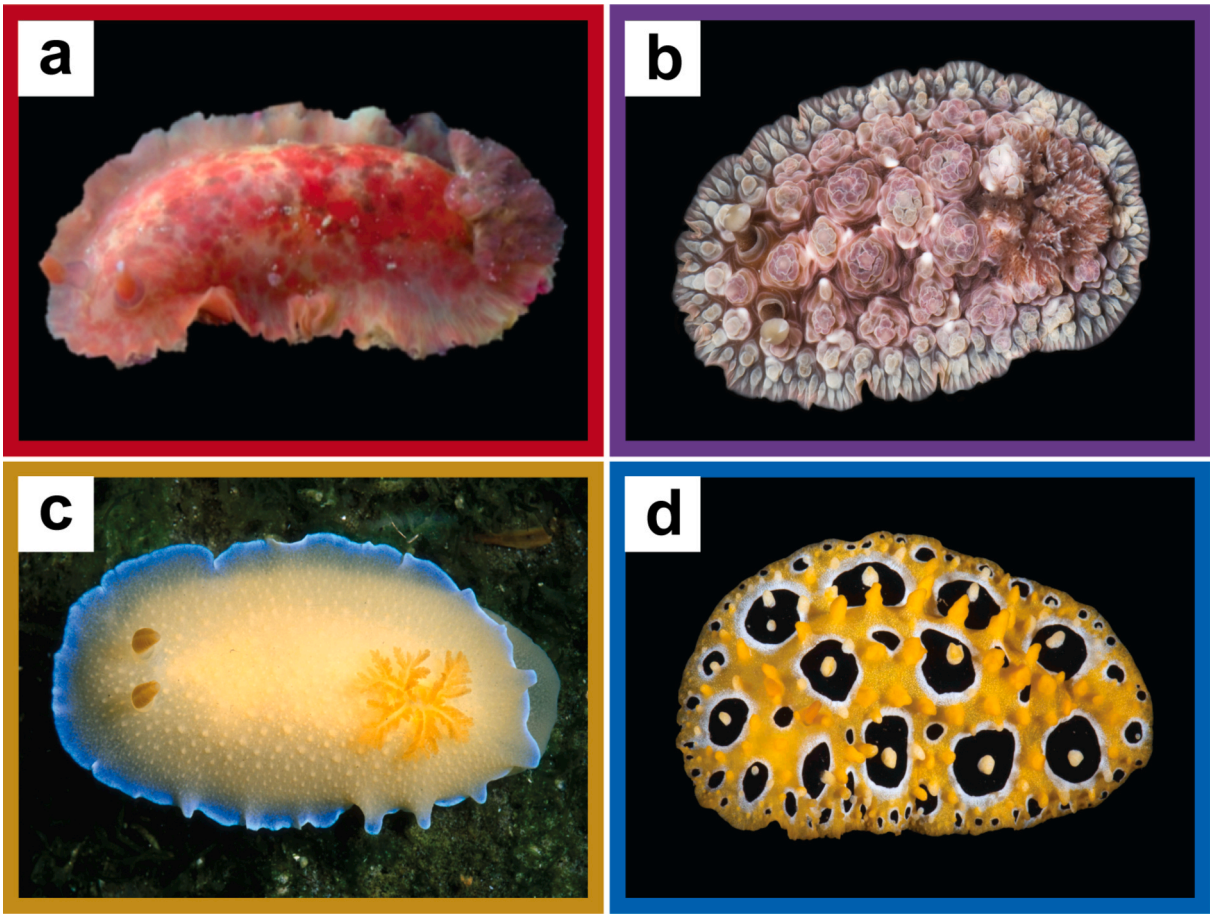


Fig. 1. Pictures of a representative species for each taxon used in the present study. (a) Smooth *Dendrodoris: Dendrodoris temarana*. Source: Carles Galià-Camps. **(b)** Warted *Dendrodoris: Dendrodoris tuberculosa*. Source: Ángel Valdés. **(c)** *Doriopsilla: Doriopsilla spaldingi*. Source: NHM Los Angeles County. **(d)** Phyllididae: *Phyllidia ocellata Source: Ángel Valdés.*

with default parameters to obtain a *de novo* assembly of the nuclear genome for each species. Mitogenome sequences were searched with BLAST against their respective nuclear genomes to filter out mitochondrial sequences. Moreover, we downloaded publicly available nuclear oxidative phosphorilation (OXPHOS) electron transfer chain genes (*cox*, *nad*, and *atp*) from the NCBI to evaluate their presence into our nuclear assemblies using BLAST. All nuclear and mitochondrial assemblies were submitted to ENA as part of the Bioproject PRJEB75450.

2.4. Mitogenome and gene characteristics

For comparison, we used the mitogenomes of *Phyllidia ocellata* and *Phyllidiella pustulosa* (NCBI accession number OP464899) from GenBank. For all species, mitogenome length and GC content was calculated with Geneious Prime. Mitochondrial genomes were aligned with MAFFT v7.376 using the L-INS-i method (Katoh and Standley, 2013), and visualized and curated in Geneious Prime. Subsequently, we compared the gene order across the mitogenome alignment.

For each mitogenome, we independently extracted both coding and ribosomal genes. We used MAFFT to carry out, gene by gene, nucleotide-based alignments of rRNA sequences and amino acid-based alignments of coding genes (CDS), with posterior manual curation. To generate nucleotide alignments of the mitochondrial coding genes, we used the software PAL2NAL v14 (Suyama et al., 2006), using as input the amino acid alignment and the unaligned nucleotide fasta file.

To evaluate mutation rates, we conducted a pairwise comparison among aligned nucleotide CDS and obtained the number of non-synonymous mutations per non-synonymous site (d*N*), synonymous mutations per synonymous site (d*S*), and their ratio (d*N*/d*S*). For this goal, we used the Maximum Likelihood method implemented in the *codeml* function of PAML v4.10.1 (Yang, 2007). For each comparison, we used a free-ratio "branch" model which allows the calculation of a distinct ratio for each branch, equilibrium codon frequencies as free parameters (*"codonfreq"* = 3), and only considered those positions without gaps to avoid ambiguous data (*"cleandata"* = 1). We implemented General Linear Models (GLM) to evaluate the factors influencing d*N*, d*S*, and d*N*/d*S*, considering gene, sequence pairwise comparison (involving or not involving smooth *Dendrodoris* (see results)), and their interaction using the function *glm* of the R package stats v4.3.1. d*N*, d*S*, and d*N*/d*S* values were log10 transformed. To further evaluate factors found to be significant, we conducted a pairwise post hoc analysis with a Tukey correction using the function *contrast* of the R package emmeans v1.10.4 (Lenth et al., 2020). We exported the results as graphs using the R package ggplot2 (Wickham et al., 2016).

2.5. OXPHOS protein structure models

To evaluate the functionality of the annotated CDS, we modeled and compared the protein structure of each CDS among Dendrodorididae morphotypes. We could not evaluate nuclear OXPHOS genes since we could not recover them in our assemblies (see results). For the mitochondrial protein coding genes we searched homolog protein templates on SWISS-MODEL (Waterhouse et al., 2018), providing as input an amino acid sequence fasta file. For each sequence, we kept the structure with the best Global Model Quality Estimate (GMQE) score to use it as reference for our protein structure model (Waterhouse et al., 2018). We

repeated the same procedure for cytochrome oxidase (*COX*) and nicotinamide adenine dinucleotide (*NAD*) protein complexes, providing as input an amino acid multifasta file including all sequences of the complex to validate that there was no aberrant structures in the protein complex assembly. The protein complex approach was not carried out for the ATP synthase (*ATP*) protein complex, since only two small subunits are synthesized in the mitochondria leaving the protein complex model largely incomplete. To evaluate structural differences among modeled proteins, we conducted pairwise comparisons among species, using the pairwise structure alignment tool with the algorithm jFATCAT (rigid) from RCSB PDB (https://www.rcsb.org/) (Duarte et al., 2022). We evaluated the percentage of sequence similarity, the average distance between the atoms of the proteins being compared, known as root-mean-square deviation of atomic positions (RMSD-value), and the topological similarity of protein structures, known as template modeling (TM)-score (Kufareva and Abagyan, 2011; Zhang and Skolnick, 2004). RMSD has an open scale, where values close to 0 indicate structure overlap at the atomic level, while the TM-score follows a 0 to 1 scale, where 1 indicates exact protein structures.

2.6. Mitochondrial phylogenies

To generate the mitochondrial phylogenies, we followed both a supermatrix and a supertree approach for both amino acid and nucleotide alignments. The supermatrix contained all CDS and the two rRNA sequences for each of the seven Dendrodoridae and the two Phyllididae species. Maximum likelihood analyses were performed with IQ-TREE2 (Minh et al., 2020). No partition was defined for amino acids phylogenetic analyses (matrix = mt_aa) (Supplementary Data 2: Table S2). For nucleotide sequences, we ran the following approaches: 1) without partitions (matrix = mt_nt_nopart, 2) partitioning each codon position per CDS + rRNA (matrix = mt_nt_codon), 3) partitioning the first and second position of the codon per CDS + rRNA (matrix = mt_nt_no3), 4) only using the first position of the codon per CDS + rRNA (matrix = mt_nt_pos1), and 5) only using the second position of the codon per CDS + rRNA (matrix = mt_nt_pos2) (Supplementary Data 2: Table S2). For the supertree, we performed maximum likelihood analyses for each CDS and rRNA without defining partitions regardless of amino acid or nucleotide sequence, and we obtained a consensus tree using ASTRAL v5.7.7 (Supplementary Data 2: Table S2) (Zhang et al., 2018). Phylogenies were visualized and customized in the iTOL5 web server (Letunic and Bork, 2021).

2.7. Nuclear genomes quality and gene features

Completeness of conserved metazoan single-copy orthologs (metazoa_odb10, 892 genes) was assessed with BUSCO v5.2.2 (Manni et al., 2021). Single-copy ortholog gene coordinates were provided by BUSCO, and were posteriorly used to retrieve nucleotide and amino acid sequences from the genome assemblies of each species with gffREAD v0.12.8 (Pertea and Pertea, 2020) Ortholog relationships of the amino acid sequences were assessed with OrthoFinder v2.5.4 using default parameters. Orthologous sequences were aligned using MAFFT and manually curated to avoid paralogs and non-reliable sequences. We kept gene alignments with all seven species present (BUSCO complete dataset).

We used PAL2NAL to obtain nucleotide alignments for the BUSCO complete dataset as described for the mitochondrial genes. We carried out pairwise comparisons to evaluate the d*N*, d*S*, and the d*N*/d*S* of the nuclear genes with the *codeml* function of PAML, using the same parameters as used for the mitochondrial genes. We did not carry out this approach on OXPHOS nuclear subunits as we could not recover them in our genome asseblies (see results). Single-copy ortholog genes d*N*, d*S*, and d*N*/d*S* values were log10 transformed and we tested differences between mitochondrial and nuclear genes using GLMs, taking into account genomic compartment (mitochondrial or nuclear), sequence pairwise comparison, and their interaction. In addition, differences among nuclear single copy-ortholog genes were also tested considering gene, sequence pairwise comparison, and their interaction. We conducted pairwise post hoc analysis with a Tukey correction using the function *contrast* of the R package emmeans. Results were exported using the R package ggplot2.

2.8. Nuclear and combined phylogenies

In addition to the BUSCO dataset containing genes from all species analyzed, we also kept single-copy ortholog gene alignments with sequences from at least four different species. With this approach, we aimed to include more genes in our analyses with a reasonable level of missing data (BUSCO partial dataset). For the phylogenies of nuclear genes, we analyzed the supermatrix with IQTREE2 and a supertree with ASTRAL on both BUSCO complete (matrix = nuc_aa_completeBUSCO) and partial datasets (matrix = nuc_aa_partialBUSCO), without partitions (Supplementary Data 2: Table S2). We then combined the mitochondrial dataset with the BUSCO complete and partial datasets to obtain a matrix with no missing data containing 13 mitochondrial and 15 nuclear genes (matrix = comb_aa_completeBUSCO), and a second matrix with more genes but a with few missing data comprising 13 mitochondrial and 81 nuclear genes (matrix = comb_aa_partialBUSCO) (Supplementary Data 2: Table S2). Supermatrix analyses were performed with IQTREE2 and supertree analysis with ASTRAL. The resulting phylogenies were visualized and customized with iTOL 5 web server.

2.9. Nuclear genes signal

We evaluated which genome assembly was best suited to be used as a pseudo-reference genome to generate a catalog of single nucleotide polymorphisms (SNPs) for all species. As a pseudo-reference genome for genotyping, we selected the best assembly based on total length and BUSCO completeness. We mapped the clean reads of the seven Dendrodoridae species to the pseudo-reference *D. tuberculosa* (see results) with bwa *mem* (Li and Durbin, 2009), and genotypes were called using the command *mpileup* in bcftools v1.16 (Danecek et al., 2021). Vcftools v0.1.17 (Danecek et al., 2011), was used to keep biallelic SNPs present in at least five of the seven species, with a minimum locus depth of 5 reads, a maximum locus depth of 100, and a minimum allele frequency of 15 % to discard species-specific loci. PLINK v1.9 (Purcell et al. 2007) was used to perform a multidimensional scaling (MDS) on the data, and the results were plotted with ggplot2 in R.

3. Results

3.1. Mitochondrial and nuclear assembly features

Illumina sequencing yielded from 8.67 Gb to 40.34 Gb per specimen (Supplementary Data 3: Table S3). After data curation, we kept from 5.96 to 38.91 Gb (Supplementary Data 3: Table S3). We successfully circularized and annotated all mitochondrial genomes, which showed no evidence of heteroplasmy. All mitochondrial genomes had the expected composition of 13 CDSs, 2 rRNAs, and 22 tRNAs with high and continuous coverage but for one to three small unresolved thymine-rich regions of ~ 20 nucleotides with a higher coverage (Supplementary Data 3: Table S3, Supplementary Data 4: Figure S1). The only exception was *D. temarana*, although its sequence was similar to *D. limbata* and therefore considered to be correct. Smooth *Dendrodoris* species had the smallest mitochondrial genome sizes, followed by *Doriopsilla*, warted *Dendrodoris*, and Phyllididae species (Fig. 2A, Supplementary Data 3: Table S3). Smooth *Dendrodoris* species had the lowest GC content, followed by *Doriopsilla*, Phyllididae, and warted *Dendrodoris* (Fig. 2A). The mitochondrial genomes alignment revealed a translocation involving the cytochrome *b* (*cob*), NADH dehydrogenase subunit I (*nad1*), and subunit 4L (*nad4l*) genes, specific for the smooth *Dendrodoris*

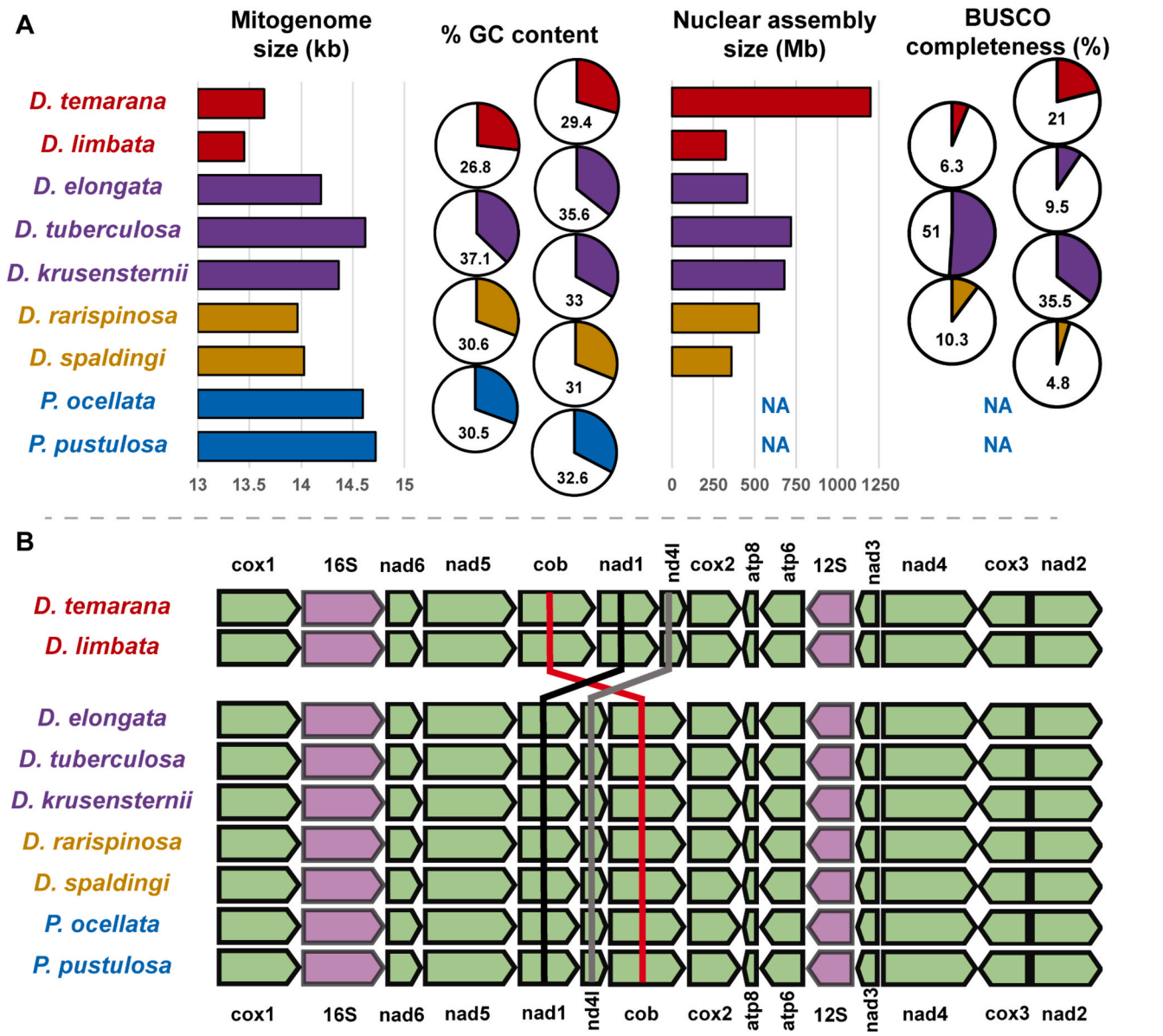


Fig. 2. Mitogenomic features of smooth *Dendrodoris* (red), warted *Dendrodoris* (purple), *Doriopsilla* (yellow), and the outgroup species Phyllididae (blue). (**A**) For each species, mitogenome assembly size (kb), %GC content, nuclear assembly size (Mb), and BUSCO completeness (%). Note that nuclear features for Phyllididae species are not available. (**B**) Mitogenomic gene order for each species studied. Black, grey, and red lines are displayed for *nad1*, *nd4l,* and *cob* respectively to facilitate mitogenome rearrangement interpretation. (For interpretation of the references to color in this figure legend, the reader is referred to the web version of this article.)

morphotype (Fig. 2B). The translocation also involved the relocation of five surrounding tRNAs. Single gene nucleotide alignments revealed numerous mutations, insertions, and deletions (indels) for both rRNA and CDS genes, most specific to the smooth *Dendrodoris* species morphotype. CDS alignments of amino acids also revealed indels and amino acid changes that distinguished smooth *Dendrodoris* from the other taxa.

Nuclear assemblies ranged from 325 Mb (*D. limbata*), to 1200 Mb (*D. temarana*) (Supplementary Data 3: Table S3). We did not detect the presence of mitochondrial pseudogenes in our nuclear assemblies using BLAST. Overall, BUSCO completeness varied with genome length, ranging from 4.8 % (43 out of 892 genes) to 51 % (455 out of 892 genes) (Supplementary Data 3: Table S3). A total of 15 genes were present in all Dendrodoridae species (BUSCO complete dataset), and 81 were present in at least four out of seven species (BUSCO partial dataset). We found no presence of the nuclear OXPHOS subunits in our nuclear assemblies (Supplementary Data 5: Table S4).

3.2. Mutation rates of mitochondrial and nuclear genes

Overall, mitochondrial genes showed higher d*N* and d*S* values than the nuclear counterparts, although this pattern was reversed for the d*N*/d*S* ratio (Fig. 3). *Dendrodoris* showed atypically high values for both synonymous and non-synonymous changes in mitochondrial genes. Interestingly, comparisons of d*N*, dS and d*N*/d*S* values involving smooth *Dendrodoris* (d*N* = 1.529 ± 2.840, d*S* = 57.228 ± 48.396, d*N*/d*S* = 0.273 ± 2.496; mean ± standard deviation) were much higher than without this morphotype (d*N* = 0.184 ± 0.172, d*S* = 42.535 ± 35.684, d*N*/d*S* = 0.009 ± 0.014) (Fig. 3). The intra-specific comparisons between the two smooth *Dendrodoris* species (*D. temarana* vs. *D. limbata*) were exceptions, with similar values to those comparisons not involving them (Supplementary Data 6: Table S5). This effect was specially evident when considering the d*N* values, as the comparison between the two smooth *Dendrodoris* returned values close to 0.1, whereas the

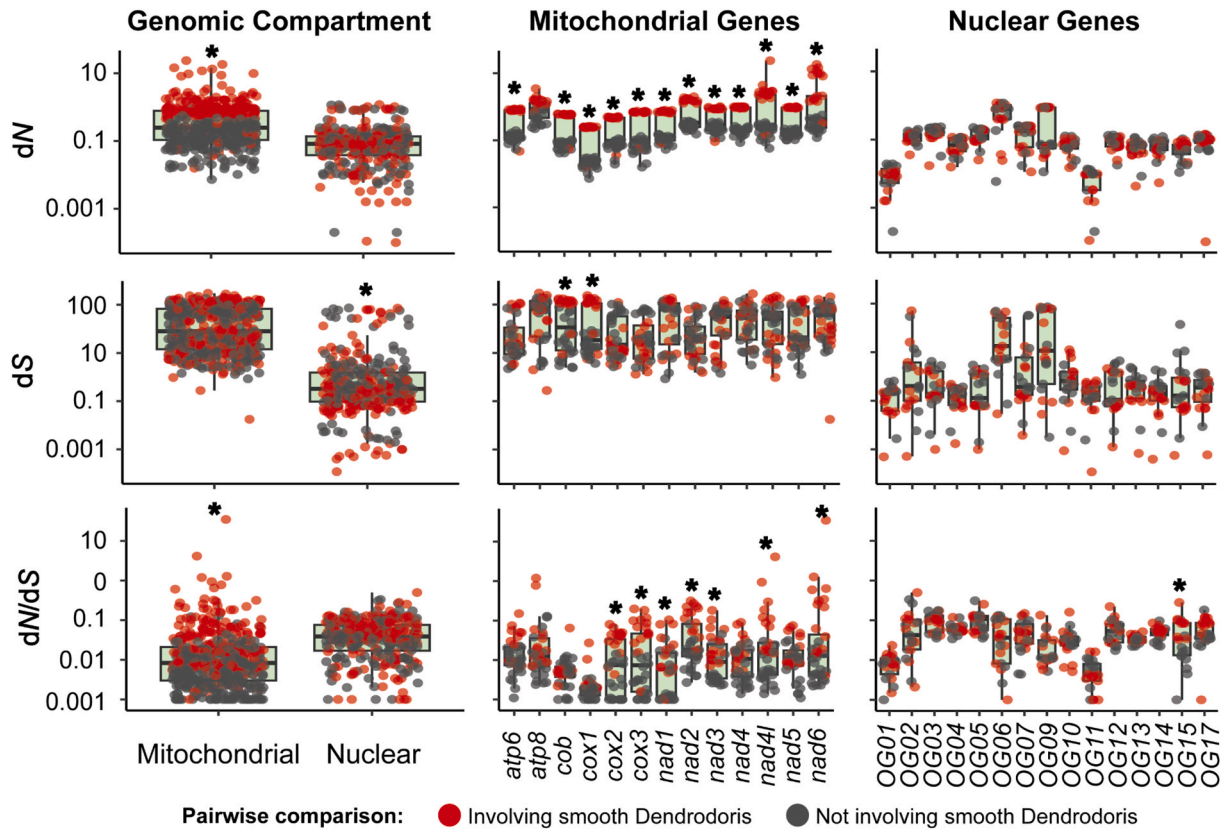


Fig. 3. d*N*, d*S*, and d*N*/d*S* values of mitochondrial and nuclear single-copy orthologous genes. The asterisks above the boxplots indicate significant differences ($p < 0.05$) after applying a Tukey post-hoc test between values involving and not involving smooth *Dendrodoris* sequences.

remaining comparisons involving smooth *Dendrodoris* species had values above 1 (Fig. 3, Supplementary Data 6: Table S5). Differences among comparisons with and without smooth *Dendrodoris* were not apparent for nuclear genes, regardless of d*N*, d*S* or d*N*/d*S* (Fig. 3, Supplementary Data 6: Table S5). Most d*N*/d*S* values involving smooth *Dendrodoris*' mitochondrial genes were below 1, except the comparison *D. temarana* vs. *P. pustulosa* on ATP synthase 8 (*atp8*) with a value of 1.19, the comparison *D. temarana* vs. *D. elongata* on *nad4l* with a value of 4.12, and the comparisons *D. temarana* vs. *P. ocellata* and *D. limbata* vs. *D. elongata* on NADH-ubiquinone oxidoreductase chain 6 (*nad6*), with values of 34.63, and 1.28 respectively. Although d*N*/d*S* values were generally larger on nuclear genes, no values above 1 were found (Fig. 3, Supplementary Data 6: Table S5).

GLMs for d*N*, d*S*, or the d*N*/d*S* ratios showed significant interactions between genome/gene and sequence comparison for all statistics (Table 1). Mitochondrial genes showed significantly higher d*N* values for those comparisons involving smooth *Dendrodoris* than without them for all genes but *atp8* (Fig. 3, Supplementary Data 7: Supp Spreadsheet). For d*S*, only *cob* and *cox1* showed significant differences between comparisons involving smooth *Dendrodoris* and without smooth *Dendrodoris*. For d*N*/d*S* ratios, cytochrome oxidase subunits 2 and 3 (*cox2*, *cox3*), NADH dehydrogenase subunits 1, 2, 3, and 4L (*nad1*, *nad2*, *nad3*, *nad4l*), and *nad6* showed differences between comparisons (Fig. 3, Supplementary Data 7: Supp Spreadsheet). When considering single-copy orthologous genes, no d*N* differences were observed. When considering all genes together, d*S* values were significantly higher for comparisons not involving smooth *Dendrodoris*, although this trend was not observed when each gene was evaluated independently (Fig. 3, Supplementary Data 7: Supp Spreadsheet). Finally, the single-copy ortholog gene *OG15* showed significantly higher d*N*/d*S* values in comparisons involving smooth *Dendrodoris* than in those not involving smooth *Dendrodoris* (Fig. 3, Supplementary Data 7: Supp Spreadsheet).

3.3. Protein structure models

Sequence identity was very low when comparing smooth *Dendrodoris* with the other two Dendrodoridae morphotypes (Table 2), with the highest value being 66 %. Nonetheless, protein models for all three main clades showed highly conserved structures for all the single genes encoded by the mitochondrial genome. For most genes, the measure of the average distance between atoms (RMSD-values) was close to 0 Angströms (Å) (Table 2), indicating a near-perfect match between Dendrodoridae protein structures. On the other hand, the topological similarity of protein structures (TM-scores) was close to 1, supporting the similarity among Dendrodoridae structures (Table 2). The exceptions to this trend were *ATP8, ND4L,* and *NAD6* with RMSD values around 2 Å and TM-scores below 0.5 (Table 2). The level of structural conservation was higher in the *COX* complex subunits than for the *NADH* or *ATP* synthase. No apparent differences in the quaternary structure were observed when the *COX* and *NADH* protein complexes were modeled (Fig. 4).

3.4. Nuclear SNPs differentiate family members

Considering the nuclear assembly length of 700 Mb and the BUSCO completeness of 51 %, we defined the genome of *D. tuberculosa* as the most comprehensive to be used as a pseudo-reference for SNP analyses. The percentage of mapping reads was highly variable depending on the species (56.08 ± 0.20 %, mean ± SD), with *D. tuberculosa* reaching the highest value (99.53 %) and *Do. rarispinosa* the lowest (39.07 %) (Supplementary Data 3: Table S3). After genotyping and filtering, we kept a total of 30,812 SNPs. The MDS separated each morphological variant, showing *Doriopsilla*, smooth *Dendrodoris,* and warted *Dendrodoris* as independent evolutionary units. The species *D. elongata* occupied an intermediate position between *Doriopsilla* and the other two warted

Table 1
General Linear Model results for the dN, dS, and dN/dS values. Note that all values were log10 transformed. We conducted two GLMs to avoid nested factors. As fixed factors we included a) Comparison (involving smooth *Dendrodoris*, not involving smooth *Dendrodoris*) and Genome (mitochondrial, nuclear), and b) Comparison and Gene. For each factor and their interaction, we provide their sum of squares (Sum Sq), degrees of freedom (DF), F value, and p-value. Significant p-values are in bold.

Statistic	Model	Factor	Sum Sq	DF	F	p-value
d*N*	Genome	Comparison	38.73	1	144.46	**<0.001**
		Genome	87.03	1	324.64	**<0.001**
		Comparison * Genome	37.19	1	138.71	**<0.001**
		Residuals	208.83	779		
	Gene	Comparison	38.61	1	355.95	**<0.001**
		Gene	210.71	27	71.95	**<0.001**
		Comparison * Gene	43.48	27	14.85	**<0.001**
		Residuals	78.85	727		
d*S*	Genome	Comparison	0.02	1	0.08	0.778
		Genome	251.10	1	885.79	**<0.001**
		Comparison * Genome	3.22	1	11.34	**0.001**
		Residuals	220.83	779		
	Gene	Comparison	0.03	1	0.11	0.737
		Gene	295.85	27	49.76	**<0.001**
		Comparison * Gene	19.22	27	3.23	**<0.001**
		Residuals	160.09	727		
d*N*/d*S*	Genome	Comparison	40.87	1	133.76	**<0.001**
		Genome	42.57	1	139.31	**<0.001**
		Comparison * Genome	18.31	1	59.93	**<0.001**
		Residuals	238.04	779		
	Gene	Comparison	40.86	1	217.46	**<0.001**
		Gene	122.98	27	24.24	**<0.001**
		Comparison * Gene	39.36	27	7.76	**<0.001**
		Residuals	136.59	727		

Dendrodoris species (Fig. 5A).

3.5. Phylogenetic analyses

3.5.1. Mitochondrial datasets

Mitochondrial trees combining CDS and rRNA data using different codon positions as partitions, showed topological differences depending on the dataset used for the analysis (Supplementary Data 2: Table S2, Fig. 5B). However, all showed a long branch for smooth *Dendrodoris* species (Supplementary Data 4: Figure S2), with bootstrap (BS) node values below 70 regardless of the analysis. When using the matrix "mit_nt_codon", *Doriopsilla* was the sister group to the smooth *Dendrodoris* clade, and warted *Dendrodoris* were the sister group of the remaining members of the family Dendrodoridae (Supplementary Data 4: Figure S2). When using the matrices "mit_nt_no3" and "mit_nt_pos2", the clade of warted *Dendrodoris* was sister to *Doriopsilla*, and the smooth *Dendrodoris* clade formed a basal polytomy with the outgroup (Supplementary Data 4: Figure S2). Finally, when using the matrix "mit_nt_pos1", smooth and warted *Dendrodoris* were sister groups, and together formed a sister group to *Doriopsilla* (Supplementary Data 4: Figure S2).

3.5.2. Nuclear datasets

The nuclear analyses revealed two topologies (Supplementary Data 2: Table S2, Supplementary Data 4: Figure S3). Both topologies supported the monophyly of smooth *Dendrodoris* and the paraphyly of warted *Dendrodoris*, with *D. elongata* as the sister clade to the remaining *Dendrodoris*. They disagree considering *D. tuberculosa* and *D. krusensternii* either as a grade ("nuc_aa_partialBUSCO_SM") or as a

Table 2
Pairwise comparison of mitochondrial protein structure models. For each protein, compared species are indicated in columns Taxon 1 and Taxon 2. For each comparison, we provide sequence identity (%), root-mean-square deviation of atomic positions in armstrongs (RMSD Å), and template modeling score (TM-score).

Protein	Taxon 1	Taxon 2	Sequence identity (%)	RMSD (Å)	TM-score
atp6	smooth *Dendrodoris*	warted *Dendrodoris*	28	1.12	0.94
	smooth *Dendrodoris*	*Doriopsilla*	30	1.14	0.94
	warted *Dendrodoris*	*Doriopsilla*	68	1.55	0.94
atp8	smooth *Dendrodoris*	warted *Dendrodoris*	19	1.57	0.37
	smooth *Dendrodoris*	*Doriopsilla*	13	2.23	0.06
	warted *Dendrodoris*	*Doriopsilla*	0	1.8	0.12
cob	smooth *Dendrodoris*	warted *Dendrodoris*	42	0.88	0.94
	smooth *Dendrodoris*	*Doriopsilla*	44	0.87	0.96
	warted *Dendrodoris*	*Doriopsilla*	85	0.61	0.97
cox1	smooth *Dendrodoris*	warted *Dendrodoris*	66	0.33	0.99
	smooth *Dendrodoris*	*Doriopsilla*	65	0.3	0.99
	warted *Dendrodoris*	*Doriopsilla*	95	0.14	0.99
cox2	smooth *Dendrodoris*	warted *Dendrodoris*	48	0.07	0.99
	smooth *Dendrodoris*	*Doriopsilla*	46	0.07	0.99
	warted *Dendrodoris*	*Doriopsilla*	85	0.04	1
cox3	smooth *Dendrodoris*	warted *Dendrodoris*	41	0.11	1
	smooth *Dendrodoris*	*Doriopsilla*	39	0.14	1
	warted *Dendrodoris*	*Doriopsilla*	84	0.11	1
nad1	smooth *Dendrodoris*	warted *Dendrodoris*	41	0.33	0.98
	smooth *Dendrodoris*	*Doriopsilla*	40	0.69	0.97
	warted *Dendrodoris*	*Doriopsilla*	76	0.66	0.99
nad2	smooth *Dendrodoris*	warted *Dendrodoris*	23	1.47	0.85
	smooth *Dendrodoris*	*Doriopsilla*	26	1.96	0.8
	warted *Dendrodoris*	*Doriopsilla*	56	2.45	0.86
nad3	smooth *Dendrodoris*	warted *Dendrodoris*	38	0.69	0.85
	smooth *Dendrodoris*	*Doriopsilla*	36	0.89	0.73
	warted *Dendrodoris*	*Doriopsilla*	64	0.85	0.85
nad4	smooth *Dendrodoris*	warted *Dendrodoris*	28	1.03	0.96
	smooth *Dendrodoris*	*Doriopsilla*	28	0.99	0.96
	warted *Dendrodoris*	*Doriopsilla*	69	0.32	0.98
nd4l	smooth *Dendrodoris*	warted *Dendrodoris*	15	2.03	0.62
	smooth *Dendrodoris*	*Doriopsilla*	16	2.34	0.59
	warted *Dendrodoris*	*Doriopsilla*	61	1.47	0.81
nad5	smooth *Dendrodoris*	warted *Dendrodoris*	32	1.12	0.91

(*continued on next page*)

Table 2 (*continued*)

Protein	Taxon 1	Taxon 2	Sequence identity (%)	RMSD (Å)	TM-score
	smooth *Dendrodoris*	*Doriopsilla*	32	1.19	0.91
	warted *Dendrodoris*	*Doriopsilla*	72	0.79	0.98
nad6	smooth *Dendrodoris*	warted *Dendrodoris*	15	1.31	0.36
	smooth *Dendrodoris*	*Doriopsilla*	17	2.57	0.39
	warted *Dendrodoris*	*Doriopsilla*	55	2.97	0.71

clade (remaining analyses), sister to smooth *Dendrodoris* (Supplementary Data 2: Table S2, Supplementary Data 4: Figure S3). *Doriopsilla* was always supported as a sister taxon to all *Dendrodoris*. All supermatrix nodes had BS values above 90, except for one node of the "nuc_aa_completeBUSCO_SM" matrix, where the support for smooth *Dendrodoris* monophyly was BS = 51 and for warted *Dendrodoris* BS = 55 (Supplementary Data 2: Table S2, Supplementary Data 4: Figure S3). The analysis of the "nuc_aa_partialBUSCO_ST" matrix recovered full support (1) for all nodes. Conversely, the phylogenetic analysis of the "nuc_aa_completeBUSCO_ST" matrix had more variable, albeit high, node support values: 0.87 for smooth *Dendrodoris*, 0.93 for warted *Dendrodoris*, and 1 for the remaining nodes (Supplementary Data 2: Table S2, Supplementary Data 4: Figure S3).

3.5.3. Combined datasets

The combined datasets inferred highly supported phylogenies, although different topologies were found (Supplementary Data 2: Table S2, Fig. 5C). Supermatrix node support was higher than supertree node support (Supplementary Data 4: Figure S4), with bootstrap values of 100 in all nodes. The only exception was the analysis of the"-comb_aa_completeBUSCO_SM" matrix, which yielded a bootstrap value of 89 for the warted *Dendrodoris* clade.

4. Discussion

With this study, we provide novel evidence for structural rearrangements and accelerated mutation events in nudibranchs. We showed that mitochondrial genes tend to contain more mutations than nuclear genes, although both have similar d*N*/d*S* ratios, indicating similar adaptive signals. However, the rearrangement of the mitogenomes of smooth *Dendrodoris* and the increased mutation rates in this group are remarkable. These mutations could have caused drastic changes in the genes contributing to the respiratory machinery with deleterious results. However, we show that despite the high mutation rates in smooth *Dendrodoris*, the overall structure of mitochondrial proteins is conserved, and therefore, their functionality is expected to be maintained. The high mutation rates in mitochondrial genes of smooth *Dendrodoris* have a direct impact on the phylogeny of the family, causing major problems in resolving the relationships between smooth *Dendrodoris* and the remaining ingroup taxa. Several previous studies have observed this mito-nuclear discordance (Hallas et al., 2017; Korshunova et al., 2020; Maniei and Wägele, 2024; Wollscheidlengeling, 2001), which has been clarified with the data and analyses presented here.

4.1. Mitochondrial gene reorganization and mutation rates

Mitochondrial structural rearrangements are hypothesized to result from duplication events followed by the random deletion of one of the

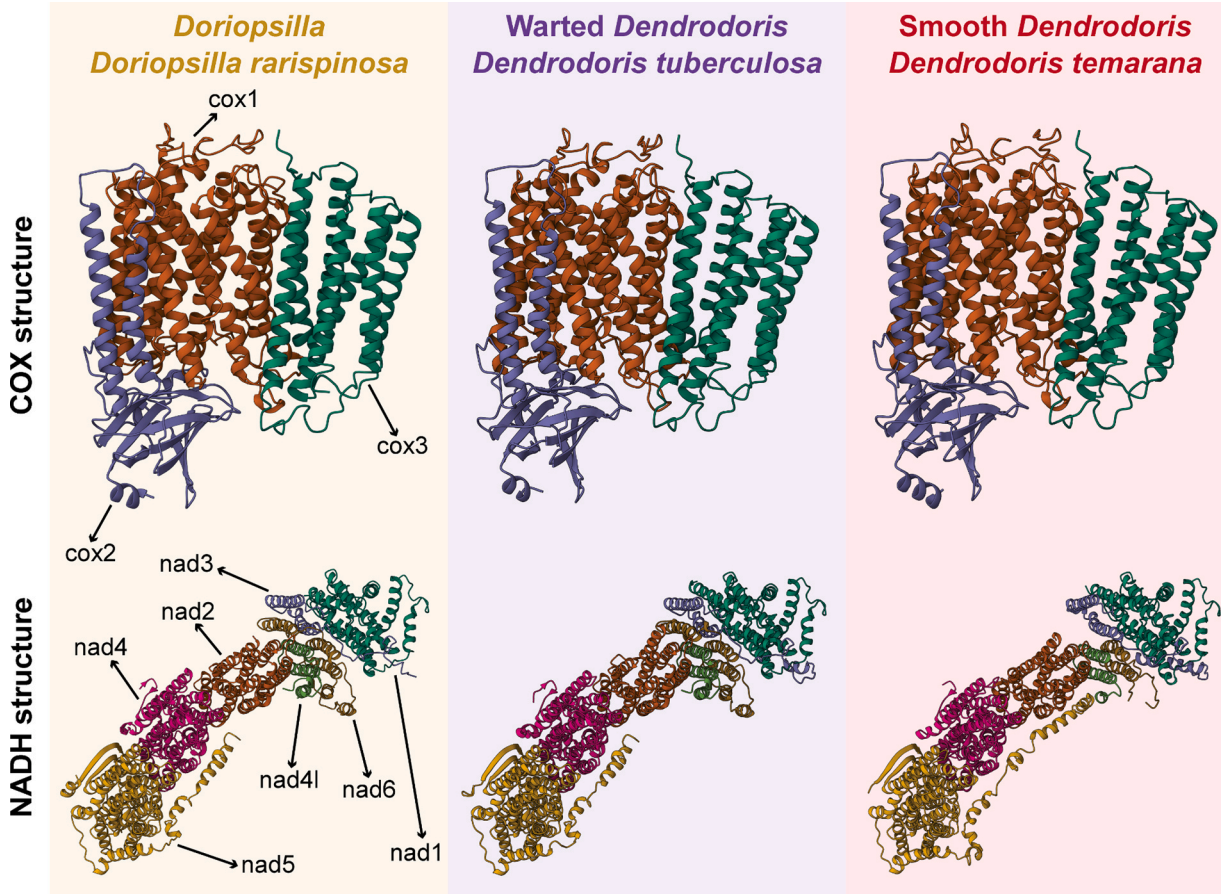


Fig. 4. Protein models obtained for the COX and NADH complexes. Each subunit of the complex is colored in a different color.

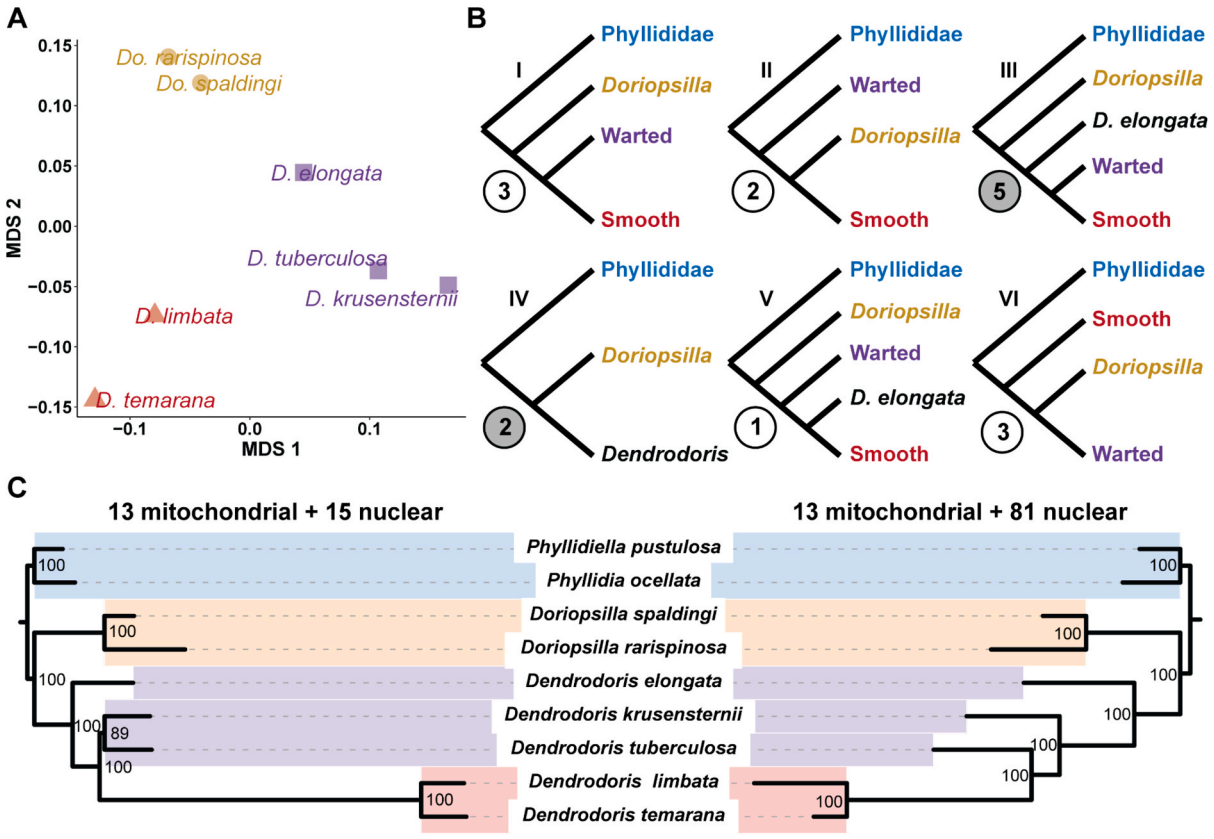


Fig. 5. Dendrodorididae systematics. **(A)** MDS analysis representation using nuclear information (30,812 SNPs) of the Dendrodorididae species. **(B)** Different topologies were obtained with the different datasets. Circled numbers indicate how many times each topology has been recovered. Gray circles indicate topologies retrieved when combining nuclear and mitochondrial data. Topology I is recovered by "mit_nt_pos1_SM", "mit_aa_ST", and "nuc_aa_partialBUSCO_ST". Topology II is recovered by "mit_nt_nopart_SM" and "mit_nt_nopart_ST". Topology III is recovered by "nuc_aa_completeBUSCO_SM", "nuc_aa_completeBUSCO_ST", "comb_aa_completeBUSCO_SM", "comb_aa_completeBUSCO_ST", and "comb_aa_partialBUSCO_ST". Topology IV is recovered by "nuc_aa_partialBUSCO_SM" and "comb_aa_partialBUSCO_SM". Topology V is recovered by "mit_aa_SM". Topology VI is recovered by "mit_nt_codon_SM", "mit_nt_no3_SM", and "mit_nt_pos2_SM".**C)** Supermatrix topologies for the combined datasets using combined matrices. Bootstrap values are reported on nodes.

copies (Françoso et al., 2023; Ghiselli et al., 2021; Shi et al., 2015). Mollusks are known for having large and structurally diverse mitochondrial genomes, with gene rearrangements occurring among distant taxa, but also at lower taxonomic levels such as within Heterobranchia (Ghiselli et al., 2021; Varney et al., 2021). Dorid nudibranchs, however, are supposed to be an exceptional case, as they are characterized by short compact mitogenomes with gene overlap (Do et al., 2022). This mitogenomic structure is thought to be relatively stable (Grande et al., 2008; Xie et al., 2019) as gene overlap accentuates the deleterious effects of mutations and rearrangements by affecting two different genes at the same time (Ghiselli et al., 2021). Thus, as mutations may simultaneously affect multiple genes, natural selection would quickly remove them, maintaining the original mitogenomic structure. Although minor mitogenome rearrangements have been already reported in nudibranchs, specifically in the genus *Hypselodoris* (Do et al., 2022), the extremely high mutation rates observed by d*N* and d*N*/d*S* values of smooth *Dendrodoris* challenge traditional views on mitochondrial genome evolution (Karagozlu et al., 2016; Varney et al., 2021). Mitochondrial genes are known to evolve faster than nuclear genes due to maternal inheritance, lack of recombination and histone proteins, as well as higher replication rates (Serrano et al., 2024). Nevertheless, our d*N* and d*S* results indicate that smooth *Dendrodoris* genes have evolved exceptionally fast in comparison to their congeneric relatives, representing the most extreme case in mollusks found to date. In fact, our average d*N*/d*S* value of 0.273 for mitochondrial genes exceed the highest observed in mollusca, that one of the asexual snail *Potamopyrgus antipodarum*, with d*N*/d*S* = 0.161, (Neiman et al., 2010). Interestingly, while most of the d*N*/d*S* values below 1 should point to purifying selection (Wang et al., 2021), the high d*S* values found for most of the mitochondrial genes of smooth *Dendrodoris* suggest that these sequences may be highly saturated (Shapiro and Alm, 2009), preventing the detection of positive selection based on d*N*/d*S* ratios. Therefore, a positive selection event occurring in the past cannot be ruled out (Shapiro and Alm, 2009).

4.2. *Protein models support orthology by functionality*

The unprecedented prevalence of non-synonymous mutations between sibling taxa in the family Dendrodorididae and the abundance of indels in all 13 CDSs + 2 rRNAs is unique among heterobranch sea slugs. Although some authors have suggested *Dendrodoris' cox1* and *16S* genes to be pseudogenes or exogenic contamination (Hallas et al., 2017; Korshunova et al., 2020), our protein subunits and protein complexes models confirm that despite having non-synonymous mutations, the protein structure is maintained. Therefore, *Dendrodoris cox1,* and by extension also *16S* genes, most likely represent functional orthologous genes. The only proteins not modeled correctly are the smallest subunits of each complex, whose deleterious effect on the entire protein complex might be negligible. Because *COX* and *NADH* protein subunits interact with each other, folding proteins such as chaperones may reduce the deleterious effects of mutation of either subunit, and the accumulation of compensatory mutations can occur (Hill, 2020; Maisnier-Patin et al., 2005). This effect can lead to a cascade of mutations in all genes involved in the protein complexes, accelerating mutation and selection

processes through synergistic epistasis (Hansen, 2013; Paixão and Barton, 2016). As a result, extremely high evolutionary rates can occur, as it has been reported in marine copepods (Stern et al., 2022). However, the mutagenesis of synergistic epistasis in mollusks is still poorly understood, and neglected in nudibranchs. However, our models should be taken cautiously as proteins were reconstructed outside of the context of the protein complex since we could not recover the OXPHOS nuclear subunits involved in *COX*, *NADH* and *ATP*. Future studies using reference genomes of Dendrodoridídae species with a broader taxon sampling should allow protein complex reconstruction and shed light on the processes leading to such genetic divergence.

4.3. Dendrodoridídae systematics and evolution

Protein models generated in the present study suggest conserved and functional protein structures, and confirm that phylogenetic studies can be effectively carried out when using mitochondrial markers, as these genes are most likely orthologous. Our phylogenetic results using mitochondrial data validate the presence of a long branch separating the smooth *Dendrodoris* clade (Hallas et al., 2017; Korshunova et al., 2020). In all cases, the phylogenetic position of the clade has a low node support value, since extremely high genetic distances between taxa makes it difficult to place this clade accurately within the family (Bergsten, 2005; Kück et al., 2012). This effect can be understood as a step-less ladder, in which the absence of intermediate forms hampers phylogenetic reconstructions. Since three deep-sea *Dendrodoris* species occur in habitats below 100 m in depth (Valdés, 2001), the inclusion of these species in future studies could provide a link between the smooth and the warted clades, which would be crucial to clarify the evolutionary history of the family Dendrodoridídae. Although we cannot establish a reliable phylogeny based on mitochondrial data due to topological inconsistencies and incomplete taxon sampling, there are sufficient indicators to support the hypothesis that smooth *Dendrodoris* should be considered as an independent evolutionary unit, sister to the rest of *Dendrodoris*. As supporting evidence, we found that the mitochondrial genetic distance is exceptionally high, as well as the presence of lineage-specific indels which can be considered as an autapomorphic syntenic trait (Schreeg et al., 2016). The difference in the mitogenome size of ~ 1000 bp and a completely different GC content: $\bar{x}$=28.10 % in smooth and $\bar{x}$=35.23 % in warted *Dendrodoris*, is consistent with morphological differences, and further confirms that these two groups of *Dendrodoris* should be considered as different genera.

The mitochondrial genome rearrangement and high mutation rates in the smooth *Dendrodoris* lineage represent the fastest evolutionary process in nudibranchs observed to date. In other groups of organisms (e.g., sauropsid reptiles), a direct correlation between rapid speciation events and accelerated evolutionary rates has been found in mitochondrial genomes (Eo and DeWoody, 2010). This scenario could explain the biodiversity of each *Dendrodoris* morphotype, since smooth *Dendrodoris* is the most speciose lineage with approximately 30 species. However, both the warted and the smooth lineages may be even more diverse, since *Dendrodoris* has been found to contain several cryptic species (Galià-Camps et al., 2022). Additionally, studies conducted in grasshopper species concluded that species subjected to weaker selection pressures on respiration had faster substitution rates than those subjected to highly demanding respiration processes (Chang et al., 2020). Warted *Dendrodoris* are commonly found below 20 m. In contrast, smooth *Dendrodoris* are found under rocks in shallow waters between 0 and 5 m depth where oxygen levels are higher, consistent with the respiratory constraint release hypothesis. Thus, the habitat of smooth *Dendrodoris*, characterized by high oxygen levels, food resources, and microhabitats, in combination with a more intense UV irradiation, could have promoted mitogenome mutation acceleration and speciation through niche specialization.

4.4. Nuclear data supports divergent evolution of smooth Dendrodoris

The generation of the first genome draft of seven Dendodoridídae species has been critical to unveil the nuclear processes underlying Dendrodoridídae evolution. It is noteworthy that our Dendrodoridídae nuclear genome drafts are still quite incomplete, as our best assembly had only 51 % of complete BUSCO genes. Considering the advance in understanding the evolution of Dendrodoridídae species using genome drafts, the potential of chromosome-level assemblies on this family and other mollusks is remarkable. The inclusion of genome-wide SNPs and sequences from nuclear coding genes has been crucial for validating the dichotomy between smooth and warted *Dendrodoris* species. All the results presented in this study point to a differentiation of smooth and warted *Dendrodoris*. Nuclear d*N*, d*S* and d*N*/d*S* results not only confirm that mitochondrial genes of smooth *Dendrodoris* evolved faster than in other Dendrodoridídae species, but also highlight that smooth *Dendrodoris* species accumulate fewer synonymous mutations in the nuclear genome than the other Dendrodoridídae species. Additionally, the SNP data supports the differentiation between smooth and warted *Dendrodoris*, as they are distinguished on the first axis of the MDS, and both groups are equally distinct from the closely related genus *Doriopsilla*. Otherwise, in a situation of large nuclear genetic distance, we should observe an extremely distant placement of the smooth *Dendrodoris* species in comparison to other family members. Similarly, the phylogenetic position of smooth *Dendrodoris* is strongly supported when nuclear data are used or combined with mitochondrial data, since low mutation rates of nuclear markers allow better inference of deeper phylogenetic nodes (Talavera and Vila, 2011). However, including more nuclear genes in the analysis directly affects the topology and thus the clusters generated. Our results support two alternative topologies. The first topology, based on 81 single-copy nuclear and 13 mitochondrial ortholog genes, supports the monophyly of the genus *Dendrodoris*, whereas the second topology, based on 15 single-copy nuclear and 13 mitochondrial genes, indicates that *Dendrodoris* could have split into three lineages. The limited taxon sampling prevented us from choosing among alternative topologies. Nonetheless, the latter phylogenetic hypothesis is in line with morphological characters, as it splits smooth and warted *Dendrodoris,* and places *D. elongata* as sister to *Doriopsilla*. *Dendrodoris elongata* has small tubercles, typical from warted *Dendrodoris*, but presents a softly spiculated mantle commonly found on *Doriopsilla* species (Furfaro et al., 2022). Thus, we encourage future taxonomic studies to revise the family Dendrodoridídae, clarify relationships among its members by using a broader taxon sampling, and perhaps officially introduce new taxonomic names for smooth *Dendrodoris*, warted *Dendrodoris*, and elongated *Dendrodoris*.

5. Conclusions

Our study has revealed accelerated evolutionary changes in the mitogenome of *Dendrodoris* species with a smooth morphotype, the second case documented in nudibranchs. Although the mechanisms behind this process and their implications for respiration remain unknown, habitat shifts might be a potential trigger for this process. We encourage future studies to expand the sampling with additional species for each morphotype and ecotype to fully resolve the systematics of the family Dendrodoridídae and better understand the selective pressures that led to the evolution of the family. In addition, future studies should include reference genome assemblies of multiple species of Dendrodoridídae. These reference genomes could fully resolve the phylogenetic relationships within the family. Moreover, they would allow the recovery of nuclear OXPHOS subunits, which would allow the study of the interactions between mitochondrial and nuclear respiratory genes, thus strengthening the knowledge behind the evolutionary processes driving smooth *Dendrodoris* mitochondrial fast evolution. Our study represents a first attempt to explore the history of the family Dendodoridídae through its mitochondrial evolution, a neglected area in

malacology but with far-reaching implications for many other taxa with diverse habitats and ecologies.

CRediT authorship contribution statement

Carles Galià-Camps: Writing – review & editing, Writing – original draft, Visualization, Validation, Software, Project administration, Methodology, Investigation, Formal analysis, Data curation, Conceptualization. **Tilman Schell:** Writing – review & editing, Validation, Supervision, Software, Resources, Data curation. **Alba Enguídanos:** Writing – review & editing, Validation, Supervision, Resources, Methodology. **Cinta Pegueroles:** Writing – review & editing, Validation, Supervision, Methodology, Investigation. **Miquel Arnedo:** Writing – review & editing, Validation, Supervision, Resources, Funding acquisition. **Manuel Ballesteros:** Writing – review & editing, Supervision, Resources, Funding acquisition, Conceptualization. **Ángel Valdés:** Writing – review & editing, Validation, Supervision, Resources, Methodology, Funding acquisition, Conceptualization. **Carola Greve:** Writing – review & editing, Validation, Supervision, Resources, Methodology, Investigation, Funding acquisition, Conceptualization.

Declaration of competing interest

The authors declare that they have no known competing financial interests or personal relationships that could have appeared to influence the work reported in this paper.

Acknowledgements

This project was funded by the Centre for Translational Biodiversity Genomics [LOEWE/1/10/519/03/03.001(0014)/52] through the program LOEWE–Landes-Offensive zur Entwicklung Wissenschaftlich-ökonomischer Exzellenz of Hesse's Ministry of Higher Education, Research, and the Arts (HMWK). Additional funding was provided by grant [PID2019-105794 GB] from Ministerio de Economía y Competitividad of Spain, the grant [PID2020-118550RB] from Ministerio de Ciencia e Innovación of Spain and the grant BlueDNA (PID2023-146307OB) funded by MCIN/AEI/10.13039/501100011033 and ERDF/EU. Partial funding was also granted with the U.S. National Science Foundation [DEB-1355177]. MA and AE are part of the [2021-SGR689] and CGC, CP, and MB are part of the [2021-SGR01271], both funded by the Agència de Gestió d'Ajudes Universitàries from the Catalonian government.

Appendix A. Supplementary material

Supplementary data to this article can be found online at https://doi.org/10.1016/j.ympev.2024.108218.

Data availability

Raw data and genome assemblies have been uploaded to the European Nucleotide Archive (ENA) under the BioProject PRJEB75450.

References

Abbott, R., Albach, D., Ansell, S., Arntzen, J.W., Baird, S.J.E., Bierne, N., Boughman, J., Brelsford, A., Buerkle, C.A., Buggs, R., Butlin, R.K., Dieckmann, U., Eroukhmanoff, F., Grill, A., Cahan, S.H., Hermansen, J.S., Hewitt, G., Hudson, A.G., Jiggins, C., Jones, J., Keller, B., Marczewski, T., Mallet, J., Martinez-Rodriguez, P., Möst, M., Mullen, S., Nichols, R., Nolte, A.W., Parisod, C., Pfennig, K., Rice, A.M., Ritchie, M.G., Seifert, B., Smadja, C.M., Stelkens, R., Szymura, J.M., Väinölä, R., Wolf, J.B.W., Zinner, D., 2013. Hybridization and speciation. J. Evol. Biol. 26, 229–246. https://doi.org/10.1111/j.1420-9101.2012.02599.x.

Bergsten, J., 2005. A review of long-branch attraction. Cladistics 21, 163–193. https://doi.org/10.1111/j.1096-0031.2005.00059.x.

Bolger, A.M., Lohse, M., Usadel, B., 2014. Trimmomatic: a flexible trimmer for Illumina sequence data. Bioinformatics. https://doi.org/10.1093/bioinformatics/btu170.

Breen, M.S., Kemena, C., Vlasov, P.K., Notredame, C., Kondrashov, F.A., 2012. Epistasis as the primary factor in molecular evolution. Nature 490, 535–538. https://doi.org/10.1038/nature11510.

Burton, R.S., 2022. The role of mitonuclear incompatibilities in allopatric speciation. Cell. Mol. Life Sci. 79, 103. https://doi.org/10.1007/s00018-021-04059-3.

Cardini, A., Thorington Jr, R.W., Polly, P.D., 2007. Evolutionary acceleration in the most endangered mammal of Canada: speciation and divergence in the Vancouver Island marmot (Rodentia, Sciuridae). J. Evol. Biol. 20, 1833–1846. https://doi.org/10.1111/j.1420-9101.2007.01398.x.

Chang, H., Qiu, Z., Yuan, H., Wang, X., Li, X., Sun, H., Guo, X., Lu, Y., Feng, X., Majid, M., Huang, Y., 2020. Evolutionary rates of and selective constraints on the mitochondrial genomes of Orthoptera insects with different wing types. Mol. Phylogenet. Evol. 145, 106734. https://doi.org/10.1016/j.ympev.2020.106734.

Cooney, C.R., Tobias, J.A., Weir, J.T., Botero, C.A., Seddon, N., 2017. Sexual selection, speciation and constraints on geographical range overlap in birds. Ecol. Lett. 20, 863–871. https://doi.org/10.1111/ele.12780.

Danecek, P., Bonfield, J.K., Liddle, J., Marshall, J., Ohan, V., Pollard, M.O., Whitwham, A., Keane, T., McCarthy, S.A., Davies, R.M., Li, H., 2021. Twelve years of SAMtools and BCFtools. GigaScience 10. https://doi.org/10.1093/gigascience/giab008.

Danecek, P., Auton, A., Abecasis, G., Albers, C.A., Banks, E., DePristo, M.A., Handsaker, R.E., Lunter, G., Marth, G.T., Sherry, S.T., McVean, G., Durbin, R., 1000 Genomes Project Analysis Group, 2011. The variant call format and VCFtools. Bioinformatics 27, 2156–2158. https://doi.org/10.1093/bioinformatics/btr330.

de Queiroz, K., 2005. Ernst Mayr and the modern concept of species. Proc. Natl. Acad. Sci. u. s. a. 102 (Suppl 1), 6600–6607. https://doi.org/10.1073/pnas.0502030102.

de Visser, J.A.G.M., Cooper, T.F., Elena, S.F., 2011. The causes of epistasis. Proc. Biol. Sci. 278, 3617–3624. https://doi.org/10.1098/rspb.2011.1537.

de Vos, J.M., Augustijnen, H., Bätscher, L., Lucek, K., 2020. Speciation through chromosomal fusion and fission in Lepidoptera. Philos. Trans. r. Soc. Lond. B Biol. Sci. 375, 20190539. https://doi.org/10.1098/rstb.2019.0539.

Dierckxsens, N., Mardulyn, P., Smits, G., 2017. NOVOPlasty: de novo assembly of organelle genomes from whole genome data. Nucleic Acids Res. 45, e18.

Do, T.D., Jung, D.-W., Kim, C.-B., 2022. Molecular phylogeny of selected dorid nudibranchs based on complete mitochondrial genome. Sci. Rep. 12, 18797. https://doi.org/10.1038/s41598-022-23400-9.

Donath, A., Jühling, F., Al-Arab, M., Bernhart, S.H., Reinhardt, F., Stadler, P.F., Middendorf, M., Bernt, M., 2019. Improved annotation of protein-coding genes boundaries in metazoan mitochondrial genomes. Nucleic Acids Res. 47, 10543–10552. https://doi.org/10.1093/nar/gkz833.

Duarte, J.M., Dutta, S., Goodsell, D.S., Burley, S.K., 2022. Exploring protein symmetry at the RCSB Protein Data Bank. Emerg Top Life Sci. https://doi.org/10.1042/ETLS20210267.

Eo, S.H., DeWoody, J.A., 2010. Evolutionary rates of mitochondrial genomes correspond to diversification rates and to contemporary species richness in birds and reptiles. Proc. Biol. Sci. 277, 3587–3592. https://doi.org/10.1098/rspb.2010.0965.

Françoso, E., Zuntini, A.R., Ricardo, P.C., Santos, P.K.F., de Souza Araujo, N., Silva, J.P. N., Gonçalves, L.T., Brito, R., Gloag, R., Taylor, B.A., Harpur, B.A., Oldroyd, B.P., Brown, M.J.F., Arias, M.C., 2023. Rapid evolution, rearrangements and whole mitogenome duplication in the Australian stingless bees Tetragonula (Hymenoptera: Apidae): A steppingstone towards understanding mitochondrial function and evolution. Int. J. Biol. Macromol. 242, 124568. https://doi.org/10.1016/j.ijbiomac.2023.124568.

Fuller, Z.L., Koury, S.A., Phadnis, N., Schaeffer, S.W., 2019. How chromosomal rearrangements shape adaptation and speciation: Case studies in Drosophila pseudoobscura and its sibling species Drosophila persimilis. Mol. Ecol. 28, 1283–1301. https://doi.org/10.1111/mec.14923.

Furfaro, G., Schreier, C., Trainito, E., Pontes, M., Madrenas, E., Girard, P., Mariottini, P., 2022. The sea slug Doriopsilla areolata Bergh, 1880 (Mollusca, Gastropoda) in the Mediterranean Sea: Another case of cryptic diversity. Diversity 14, 297. https://doi.org/10.3390/d14040297.

Galià-Camps, C., Cervera, J.L., Valdés, Á., Ballesteros, M., 2022. Attack on crypsis: Molecular and morphological study of Dendrodoris Ehrenberg, 1831 (Mollusca: Gastropoda: Nudibranchia) from the Mediterranean Sea and Northern Atlantic Ocean reinstates Dendrodoris temarana Pruvot-Fol, 1953. Zootaxa. https://doi.org/10.11646/zootaxa.5133.3.4.

Ghiselli, F., Maurizii, M.G., Reunov, A., Ariño-Bassols, H., Cifaldi, C., Pecci, A., Alexandrova, Y., Bettini, S., Passamonti, M., Franceschini, V., Milani, L., 2019. Natural Heteroplasmy and Mitochondrial Inheritance in Bivalve Molluscs. Integr. Comp. Biol. 59, 1016–1032. https://doi.org/10.1093/icb/icz061.

Ghiselli, F., Gomes-Dos-Santos, A., Adema, C.M., Lopes-Lima, M., Sharbrough, J., Boore, J.L., 2021. Molluscan mitochondrial genomes break the rules. Philos. Trans. r. Soc. Lond. B Biol. Sci. 376, 20200159. https://doi.org/10.1098/rstb.2020.0159.

Grande, C., Templado, J., Zardoya, R., 2008. Evolution of gastropod mitochondrial genome arrangements. BMC Evol. Biol. 8, 61. https://doi.org/10.1186/1471-2148-8-61.

Hallas, J.M., Chichvarkhin, A., Gosliner, T.M., 2017. Aligning evidence: concerns regarding multiple sequence alignments in estimating the phylogeny of the Nudibranchia suborder Doridina. R Soc Open Sci 4, 171095. https://doi.org/10.1098/rsos.171095.

Hansen, T.F., 2013. Why epistasis is important for selection and adaptation. Evolution 67, 3501–3511. https://doi.org/10.1111/evo.12214.

Hill, G.E., 2016. Mitonuclear coevolution as the genesis of speciation and the mitochondrial DNA barcode gap. Ecol. Evol. 6, 5831–5842. https://doi.org/10.1002/ece3.2338.

Hill, G.E., 2020. Mitonuclear Compensatory Coevolution. Trends Genet. 36, 403–414. https://doi.org/10.1016/j.tig.2020.03.002.
Johnson, M.S., Reddy, G., Desai, M.M., 2023. Epistasis and evolution: recent advances and an outlook for prediction. BMC Biol. 21, 120. https://doi.org/10.1186/s12915-023-01585-3.
Karagozlu, M.Z., Sung, J., Lee, J., Kwak, W., Kim, C.-B., 2016. Complete sequences of mitochondrial genome of (A. Adams, 1861) (Mollusca, Gastropoda, Nudibranchia). Mitochondrial DNA B Resour 1, 266–267. https://doi.org/10.1080/23802359.2016.1159933.
Katoh, K., Standley, D.M., 2013. MAFFT multiple sequence alignment software version 7: improvements in performance and usability. Mol. Biol. Evol. 30, 772–780. https://doi.org/10.1093/molbev/mst010.
Korshunova, T., Fletcher, K., Picton, B., Lundin, K., Kashio, S., Sanamyan, N., Sanamyan, K., Padula, V., Schrödl, M., Martynov, A., 2020. The Emperor's Cadlina, hidden diversity and gill cavity evolution: new insights for the taxonomy and phylogeny of dorid nudibranchs (Mollusca: Gastropoda). Zool. J. Linn. Soc. 189, 762–827. https://doi.org/10.1093/zoolinnean/zlz126.
Kück, P., Mayer, C., Wägele, J.-W., Misof, B., 2012. Long branch effects distort maximum likelihood phylogenies in simulations despite selection of the correct model. PLoS One 7, e36593.
Kufareva, I., Abagyan, R., 2011. Methods of Protein Structure Comparison. Methods Mol. Biol. https://doi.org/10.1007/978-1-61779-588-6_10.
Lenth, R., Singmann, H., Love, J., Buerkner, P., Herve, M., 2020. emmeans: estimated marginal means. R package version 1.4. 4. Am. Stat.
Letunic, I., Bork, P., 2021. Interactive Tree Of Life (iTOL) v5: an online tool for phylogenetic tree display and annotation. Nucleic Acids Res. 49, W293–W296. https://doi.org/10.1093/nar/gkab301.
Li, H., Durbin, R., 2009. Fast and accurate short read alignment with Burrows-Wheeler transform. Bioinformatics 25, 1754–1760. https://doi.org/10.1093/bioinformatics/btp324.
Maisnier-Patin, S., Roth, J.R., Fredriksson, A., Nyström, T., Berg, O.G., Andersson, D.I., 2005. Genomic buffering mitigates the effects of deleterious mutations in bacteria. Nat. Genet. 37, 1376–1379. https://doi.org/10.1038/ng1676.
Maniei, F., Wägele, H., 2024. Dendrodorididae (Heterobranchia, Nudibranchia) from Persian Gulf with a description of a new species of Doriopsilla and remarks on the family. Eur. J. Taxon. 943. https://doi.org/10.5852/ejt.2024.943.2595.
Manni, M., Berkeley, M.R., Seppey, M., Zdobnov, E.M., 2021. BUSCO: Assessing Genomic Data Quality and Beyond. Curr Protoc 1, e323.
Marques, D.A., Lucek, K., Sousa, V.C., Excoffier, L., Seehausen, O., 2019. Admixture between old lineages facilitated contemporary ecological speciation in Lake Constance stickleback. Nat. Commun. 10, 4240. https://doi.org/10.1038/s41467-019-12182-w.
Mayjonade, B., Gouzy, J., Donnadieu, C., Pouilly, N., Marande, W., Callot, C., Langlade, N., Muños, S., 2016. Extraction of high-molecular-weight genomic DNA for long-read sequencing of single molecules. Biotechniques 61, 203–205. https://doi.org/10.2144/000114460.
Mendelson, T.C., Safran, R.J., 2021. Speciation by sexual selection: 20 years of progress. Trends Ecol. Evol. 36, 1153–1163. https://doi.org/10.1016/j.tree.2021.09.004.
Minh, B.Q., Schmidt, H.A., Chernomor, O., Schrempf, D., Woodhams, M.D., von Haeseler, A., Lanfear, R., 2020. IQ-TREE 2: New Models and Efficient Methods for Phylogenetic Inference in the Genomic Era. Mol. Biol. Evol. 37, 1530–1534. https://doi.org/10.1093/molbev/msaa015.
Neiman, M., Hehman, G., Miller, J.T., Logsdon Jr, J.M., Taylor, D.R., 2010. Accelerated mutation accumulation in asexual lineages of a freshwater snail. Mol. Biol. Evol. 27, 954–963. https://doi.org/10.1093/molbev/msp300.
Nowak, K., Cardini, A., Elton, S., 2008. Evolutionary Acceleration and Divergence in Procolobus kirkii. International Journal of Primatology. doi: 10.1007/s10764-008-9313-2.
Omilian, A.R., Taylor, D.J., 2001. Rate acceleration and long-branch attraction in a conserved gene of cryptic daphniid (Crustacea) species. Mol. Biol. Evol. 18, 2201–2212. https://doi.org/10.1093/oxfordjournals.molbev.a003767.
Paixão, T., Barton, N.H., 2016. The effect of gene interactions on the long-term response to selection. Proc. Natl. Acad. Sci. u. s. a. 113, 4422–4427. https://doi.org/10.1073/pnas.1518830113.
Pertea, G., Pertea, M., 2020. GFF utilities. GffRead and GffCompare. F1000Res. 9, 304. https://doi.org/10.12688/f1000research.23297.1.
Phillips, P.C., 2008. Epistasis–the essential role of gene interactions in the structure and evolution of genetic systems. Nat. Rev. Genet. 9, 855–867. https://doi.org/10.1038/nrg2452.
Prjibelski, A., Antipov, D., Meleshko, D., Lapidus, A., Korobeynikov, A., 2020. Using SPAdes De Novo Assembler. Curr. Protoc. Bioinformatics 70, e102.
Řezáč, M., Arnedo, M.A., Opatova, V., Musilová, J., Řezáčová, V., Král, J., 2018. Taxonomic revision and insights into the speciation mode of the spider Dysdera erythrina species-complex (Araneae : Dysderidae): sibling species with sympatric distributions. Invertebr. Syst. 32, 10. https://doi.org/10.1071/is16071.
Schluter, D., Rieseberg, L.H., 2022. Three problems in the genetics of speciation by selection. Proc. Natl. Acad. Sci. u. s. a. 119. https://doi.org/10.1073/pnas.2122153119 e2122153119.
Schreeg, M.E., Marr, H.S., Tarigo, J.L., Cohn, L.A., Bird, D.M., Scholl, E.H., Levy, M.G., Wiegmann, B.M., Birkenheuer, A.J., 2016. Mitochondrial Genome Sequences and Structures Aid in the Resolution of Piroplasmida phylogeny. PLoS One 11, e0165702.
Serrano, I.M., Hirose, M., Valentine, C.C., Roesner, S., Schmidt, E., Pratt, G., Williams, L., Salk, J., Ibrahim, S., Sudmant, P.H., 2024. Mitochondrial haplotype and mito-nuclear matching drive somatic mutation and selection throughout ageing. Nat Ecol Evol 8, 1021–1034. https://doi.org/10.1038/s41559-024-02338-3.
Shapiro, B.J., Alm, E., 2009. The slow:fast substitution ratio reveals changing patterns of natural selection in gamma-proteobacterial genomes. ISME J. 3, 1180–1192. https://doi.org/10.1038/ismej.2009.51.
Shi, W., Gong, L., Wang, S.-Y., Miao, X.-G., Kong, X.-Y., 2015. Tandem Duplication and Random Loss for mitogenome rearrangement in Symphurus (Teleost: Pleuronectiformes). BMC Genomics 16, 355. https://doi.org/10.1186/s12864-015-1581-6.
Stern, D.B., Anderson, N.W., Diaz, J.A., Lee, C.E., 2022. Genome-wide signatures of synergistic epistasis during parallel adaptation in a Baltic Sea copepod. Nat. Commun. 13, 4024. https://doi.org/10.1038/s41467-022-31622-8.
Sutovsky, P., 2019. Cellular and Molecular Basis of Mitochondrial Inheritance: Mitochondrial Disease and Fitness. Springer.
Suyama, M., Torrents, D., Bork, P., 2006. PAL2NAL: robust conversion of protein sequence alignments into the corresponding codon alignments. Nucleic Acids Res. 34, W609–W612. https://doi.org/10.1093/nar/gkl315.
Talavera, G., Vila, R., 2011. What is the phylogenetic signal limit from mitogenomes? The reconciliation between mitochondrial and nuclear data in the Insecta class phylogeny. BMC Evol. Biol. 11, 315. https://doi.org/10.1186/1471-2148-11-315.
Teske, P.R., Sandoval-Castillo, J., Golla, T.R., Emami-Khoyi, A., Tine, M., von der Heyden, S., Beheregaray, L.B., 2019. Thermal selection as a driver of marine ecological speciation. Proc. Biol. Sci. 286, 20182023. https://doi.org/10.1098/rspb.2018.2023.
Tobler, M., Barts, N., Greenway, R., 2019. Mitochondria and the Origin of Species: Bridging Genetic and Ecological Perspectives on Speciation Processes. Integr. Comp. Biol. 59, 900–911. https://doi.org/10.1093/icb/icz025.
Varney, R.M., Brenzinger, B., Malaquias, M.A.E., Meyer, C.P., Schrödl, M., Kocot, K.M., 2021. Assessment of mitochondrial genomes for heterobranch gastropod phylogenetics. BMC Ecol Evol 21, 6. https://doi.org/10.1186/s12862-020-01728-y.
Visinoni, F., Delneri, D., 2022. Mitonuclear interplay in yeast: from speciation to phenotypic adaptation. Curr. Opin. Genet. Dev. 76, 101957. https://doi.org/10.1016/j.gde.2022.101957.
Wang, X., Zhou, S., Wu, X., Wei, Q., Shang, Y., Sun, G., Mei, X., Dong, Y., Sha, W., Zhang, H., 2021. High-altitude adaptation in vertebrates as revealed by mitochondrial genome analyses. Ecol. Evol. 11, 15077–15084. https://doi.org/10.1002/ece3.8189.
Waterhouse, A., Bertoni, M., Bienert, S., Studer, G., Tauriello, G., Gumienny, R., Heer, F. T., de Beer, T.A.P., Rempfer, C., Bordoli, L., Lepore, R., Schwede, T., 2018. SWISS-MODEL: homology modelling of protein structures and complexes. Nucleic Acids Res. 46, W296–W303. https://doi.org/10.1093/nar/gky427.
Wellenreuther, M., Svensson, E.I., Hansson, B., 2014. Sexual selection and genetic colour polymorphisms in animals. Mol. Ecol. 23, 5398–5414. https://doi.org/10.1111/mec.12935.
Wickham, H., Chang, W., Wickham, M.H., 2016. Package "ggplot2". Create elegant data visualisations using the grammar of graphics. Version 2, 1–189.
Wollscheidlengeling, E., 2001. The phylogeny of Nudibranchia (Opisthobranchia, Gastropoda, Mollusca) reconstructed by three molecular markers. Org. Divers. Evol. 1, 241–256. https://doi.org/10.1078/1439-6092-00022.
Xiang, P., Lin, M., Wang, Y., Shen, K.-N., Hsiao, C.-D., 2016. The complete mitogenome of sea slug, (Mollusca: Phyllidiidae). Mitochondrial DNA B Resour 1, 96–97. https://doi.org/10.1080/23802359.2015.1137842.
Xie, G.-L., Köhler, F., Huang, X.-C., Wu, R.-W., Zhou, C.-H., Ouyang, S., Wu, X.-P., 2019. A novel gene arrangement among the Stylommatophora by the complete mitochondrial genome of the terrestrial slug Meghimatium bilineatum (Gastropoda, Arionoidea). Mol. Phylogenet. Evol. 135, 177–184. https://doi.org/10.1016/j.ympev.2019.03.002.
Yang, Z., 2007. PAML 4: phylogenetic analysis by maximum likelihood. Mol. Biol. Evol. 24, 1586–1591. https://doi.org/10.1093/molbev/msm088.
Zhang, C., Rabiee, M., Sayyari, E., Mirarab, S., 2018. ASTRAL-III: polynomial time species tree reconstruction from partially resolved gene trees. BMC Bioinf. 19, 153. https://doi.org/10.1186/s12859-018-2129-y.
Zhang, Y., Skolnick, J., 2004. Scoring function for automated assessment of protein structure template quality. Proteins 57, 702–710. https://doi.org/10.1002/prot.20264.